Egypt. J. Chem. **Vol. 68**, No. 5 pp. 617 - 632 (2025)

Egyptian Journal of Chemistry

http://ejchem.journals.ekb.eg/

Effect of Recycled Tungsten Carbide on the Mechanical, Physical, and Tribological Performance of Copper-Based Composites

Ahmed O. Abdel-Mawla [a] *, Samy Zein El-Abden [b], G. Abouelmagd [b], Omayma A. El-Kady [a]

[a] *Powder Technology Department, Manufacturing Technology Institute CMRDI, Cairo, Egypt*

[b] *Professor, Department of Production Engineering and Mechanical Design, Faculty of Engineering, Minia University, Minia, Egypt*

Abstract

This study comprehensively explores the effect of reinforcing a copper matrix with recycled tungsten carbide (RWC) powder to enhance its mechanical and tribological properties. The copper matrix was initially fortified with fixed proportions of 8 wt.% high-carbon ferrochromium (HC-FeCr), 20 wt. % iron (Fe), 10 wt.% graphite (C), and 2 wt.% molybdenum disulfides (MoS2) via high-energy mechanical milling. Recycled tungsten carbide (RWC) powder in varying concentrations (1-5 wt.%) was subsequently blended with the matrix for 6 hours at 200 rpm. Graphite, MoS2, and RWC surface modification was achieved through nano-copper coating via electroless chemical deposition. The composite powders were consolidated using a hot-press technique at 1010°C under 15 MPa for 15 minutes. The study's comprehensive characterization included density, XRD, SEM analysis, hardness, wear, friction coefficient assessments, and electrical and thermal conductivity measurements. The results revealed a 25% increase in hardness and a 12% reduction in wear rate with the addition of WC, alongside a gradual decline in the friction coefficient. However, the electrical and thermal conductivities diminished as RWC content increased. The Abbott-firestone curves show enhancement in the exploitation zone from (88 – 96%) at load 0.4 MPa and from (84-93%) at load 0.7 MPa.

Keywords: Copper composite, Recycled tungsten carbide, Powder metallurgy, Hot-press, Surface roughness, The Abbott firestone.

1. Introduction

Tungsten carbide was famed as one of the best and most extensively utilized ceramic reinforcements for copper matrix composites since it can improve hardness and wear resistance, making it a common ingredient in producing wear-resistant materials [1]. Copper composites are promising because they combine ductility, low density, high thermal and electrical properties, high mechanical strength, toughness at high temperatures, and increased stiffness. As a result, it has numerous industrial applications, including friction materials in various transportation machines for steady and safe deceleration or braking, antennae, vehicle piston crowns, electrical superconductors, contacts, filaments, and electrodes [2]. Several researchers have investigated using tungsten carbide as a reinforcing phase for copper matrix. Girish B.M. concluded that blending tungsten carbide particles into the copper matrix improved the mechanical properties of the composites while slightly increasing the electrical resistance [3]. Lu Han fabricated a Cu matrix with WC nanoparticles using electrodeposition and spark plasma sintering. The formed composites have high thermal stability and improved mechanical performance, making them suitable for applications as a heat sink material [4] Through the stir-casting process, Rajesh D. investigated the mechanical properties of tungsten carbide-reinforced aluminum metal matrix composites. The hardness and tensile strength were increased with the weight fraction of tungsten carbide up to 3%, after which they started to decrease due to the aggregation of WC particles that hindered the increase in hardness and tensile strength [5]. Dingdong Gu investigated the microstructures and properties of tungsten carbide (WC) particle-reinforced copper (Cu) matrix composites produced by direct metal laser sintering (DMLS) with the addition of rare earth (RE) elements. D. Gu et al. have stated an enhancement in the mechanical characteristic, with a friction coefficient of 0.8, a densification level of 95.7%, a microhardness of 417.6 HV, and a fracture strength of 201.8 MPa [6]. Vidyuk et al. investigated the synthesis of tungsten carbides in a copper matrix using spark plasma sintering (SPS), emphasizing the impact of processing conditions on microstructure and properties. Milling for 10 minutes and sintering at 980°C achieved complete tungsten carbide formation, resulting in a WC–W_2C–Cu composite with Cu-rich regions and submicron carbide particles. The material exhibited remarkable properties, including 300 HV hardness, 24% IACS electrical conductivity, and <5% porosity. This innovative approach highlights the potential of combining mechanical milling and SPS to produce nanostructured composites with superior wear resistance. The findings demonstrate advanced techniques' effectiveness in engineering high-performance metal-matrix composites [7]. Ahmadian et al. explored

*Corresponding author e-mail: engahmedosama114@gmail.com.; (Ahmed O. Abdel-Mawla).
Received date 22 January 2025; Revised date 27 February 2025; Accepted date 10 March 2025
DOI: 10.21608/ejchem.2025.354763.11199
©2025 National Information and Documentation Center (NIDOC)

ways to enhance copper-based composites by reinforcing them with nano-sized silicon carbide (SiC) and multi-walled carbon nanotubes (MWCNTs) using powder metallurgy and spark plasma sintering (SPS). The results showed that adding these reinforcements led to smaller particle and crystallite sizes, improved hardness, and better wear resistance. Also, there is a reduction in thermal conductivity and electrical conductivity, especially in the Cu-5%SiC-1%MWCNT composite[8].

Sadoun et al. investigated the effects of alumina coating with silver on the mechanical and tribological properties of Al_2O_3-reinforced copper matrix nanocomposites. They fabricated composites with varying alumina content (2.5–10 wt%) using mechanical alloying and powder metallurgy. Their findings showed that increasing Al_2O_3 content enhanced hardness, reaching a maximum of 175 HV, and significantly reduced abrasive wear rates due to the rigid ceramic reinforcement. However, densification decreased as alumina content increased. The study highlights the potential of silver-coated alumina to improve wear resistance and mechanical performance in copper-based composites[9].

Adding self-lubricating elements like graphite and MoS_2 to Cu composites is helpful for mechanical applications that call for low friction coefficients, such as bearings. However, as their ceramic nature differs from Cu's metallic nature, both are regrettably non-wettable in a Cu matrix. This issue can be resolved by reducing the surface energy and improving the interfacial bonding between them and Cu. A copper nanometallic layer can be applied to their surfaces to accomplish this.

This study aims to enhance the copper (Cu) matrix by incorporating recycled tungsten carbide (RWC) powder. Along with the schematic of our experimental design in Figure 1, the Cu composite with coated reinforcement was developed to create a material suitable for mechanical and industrial applications. Additionally, this approach addresses the non-wettability issue between the reinforcement and the Cu matrix.

2. Experimental work

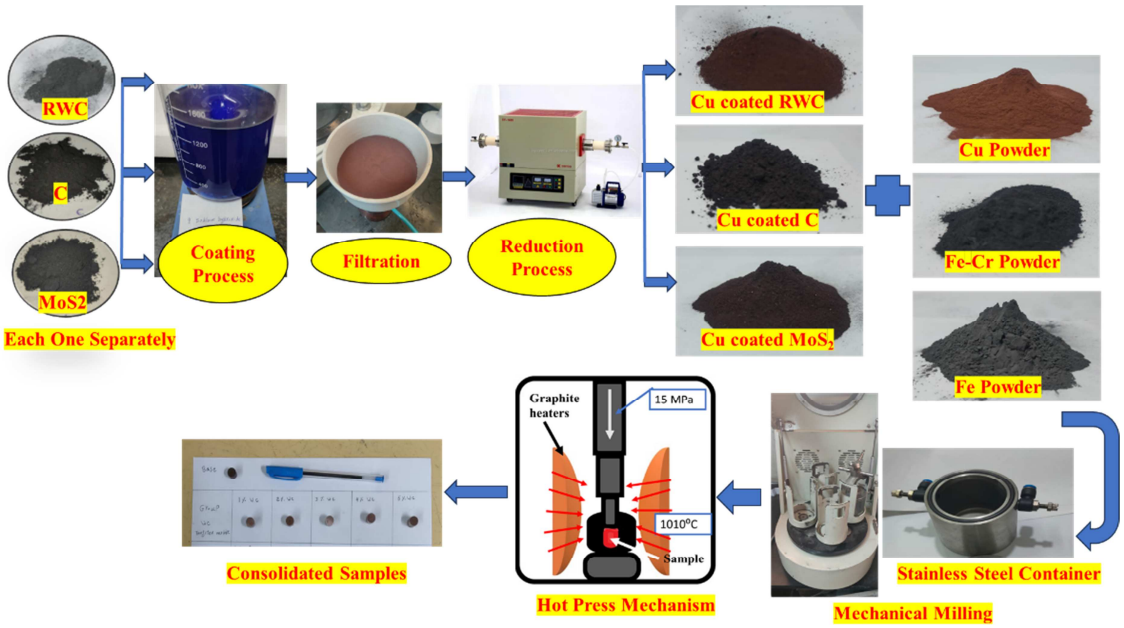

Figure (1): Schematic of the experimental process for sample preparation.

2.1. Specifications of raw materials

-The as-received elementary powders

Cu is used as a base metal matrix to prepare a composite material; iron and high-carbon ferrochromium alloys are added as alloying elements to increase the mechanical properties. Graphite and molybdenum disulfide are used as self-lubricant materials. Table (1) shows the specifications of the used metals and materials.

The recycled tungsten carbide powder (RWC)

As mentioned in the study by Ahmed O. Abdel-Mawla, recycled tungsten carbide powder is prepared by the direct recycling zinc melt process and is utilized as a reinforcing material [10].

The P30 ISO designation for the virgin tungsten carbide sample used in the recycling process indicates that its chemical composition is 5% TiC, 2% (NbC, TaC), 9% Co, and 84% WC.

Table (2) presents the XRF analysis of the RWC powder. The results demonstrate the effectiveness of the recycling process, with tungsten carbide recovered at a high purity rate of around 98% and a semi-sphere-shaped particle size range of 430 nm to 3 µm, as depicted in Figure (2).

Table (1): The specifications and source of all used materials.

Material	Particle size	Purity	Supplier
Copper (Cu)	<75 µm	99.7%	Oxford, Lab Fine Chem, India
Iron (Fe)	<75 µm	99.5%	
Graphite (C)	<90 µm	99.5%	Srlchem, India
Molybdenum Disulphide (MoS_2)	<50 µm	99%	
Silicon (Si)	<100 µm	99.5%	
Chromium (Cr)	<150 µm	99%,	

Table (2): The XRF of RWC and virgin powders.

Analyte	Virgin powder (wt.%)	Recycled Powder (wt.%)
Ti	5.262	3.712
Fe	0.249	1.08
Co	9.724	6.796
Zn	0	0.043
Nb	0.867	0.903
Ta	0.963	1.063
W	75.2295	81.569
C	6.365	4.3

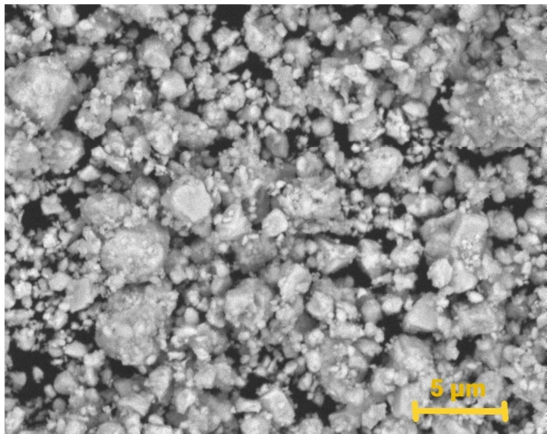

Figure (2): SEM of the recycling tungsten carbide powder

2.2. Preparation of the composite samples

2.2.1. Coating of ceramic powders by electro-less chemical deposition

An electroless chemical deposition process has been applied to improve the wettability between the ceramic particles, such as RWC, MoS_2, and graphite, and the metallic copper matrix[11]. The electroless plating method involves coatings from metallic ion solutions without needing any external electrical energy source. It is used to capsulate conductive or nonconductive materials on a powder surface by a nanometallic layer such as Cu, Ag, or Ni to decrease the surface energy with another surface. Copper (II) sulfate pentahydrate, sodium hydroxide (Pellets, Purity 98%, India), potassium sodium tartrate (Rochel salt) (Powder, Purity 99%, Egypt), and formaldehyde (Solution, Assay 38%, Egypt) bath was used. The surface of each powder was activated by a magnetic stirrer with a 10% NaOH solution for one hour; after that, the powders were filtered, washed with distilled water, and dried. After the activation process, each powder (recycling tungsten carbide, graphite, and molybdenum disulfide) was added separately to the copper deposition chemical bath, which is composed of 43.75 g of $CuSO_4.5H_2O$ dissolved in 1250 ml distilled water, then 62.5 g of NaOH was added (as a PH adjusting material), 150 g of $KNaC_4H_4O.4H2O$, and 250 ml/l formaldehyde (as a reducing agent). The reaction was immediately initiated by adding the formaldehyde and adjusting the PH~12. The reaction was completed after 1 hour by coating a Cu layer on the surface of the above-mentioned ceramic materials. So, their capsulation was established by a nano Cu-layer.

The powders were filtered, washed with distilled water, and dried in a muffle furnace at 80 C for 1 hour. Finally, the Cu-coated powders undergo a hydrogen reduction cycle in a gas tube furnace at 500 C for 1 hour to remove any oxidation in the copper particles [12]. Because the electroless chemical deposition method takes place in an aqueous solution, the deposited Cu was in the form of CuO. So, the reduction step is essential to obtain a nano Cu layer.

2.2.2. Preparation of the high carbon ferrochromium alloy by mechanical alloying

Ferro-chromium was added to the copper matrix with a constant ratio to enhance the wear resistance of the composite. The chemical composition of the Fe-Cr powder is given in Table (3).

Table (3): Chemical composition of the Fe-Cr powder in wt.%.

Element	Cr	Fe	Si	C
Concentration wt.%	64	27.36	1.8	6.84

All the proportions indicated in the above Table were mixed mechanically for 50 hours with a speed of 250 rpm by the planetary ball mill model (PQ-N2) with a 5:1 ball-to-powder ratio in the presence of argon gas to protect the elements from any oxidation in which the ferrochromium alloy was formed [13], as detected by XRD.

2.3. Preparation of copper composite sample

The composition of the copper matrix in weight percentage was 20% Fe, 10% copper-coated graphite, 8% FeCr, 2% copper-coated MoS_2, and 60 % Cu. The copper-coated recycled tungsten carbide powder was added to the above copper matrix as a reinforcement material from 0 to 5 wt.% by one interval.

The ratios mentioned above were mixed mechanically with the different percentages of the recycled tungsten carbide powder using a planetary ball mill for 6 hours at 200 rpm speed with a 4:1 ball-to-powder ratio. 1.5 wt. % hexane was added during milling as a process controlling agent (PCA) [14].

2.4. Samples consolidation

Consolidation of the samples was carried out in a Vertical Vacuum Hot Press Furnace (Model HIQ-22HP), under pressure of 15 MPa at a temperature of 1010° C for 15 minutes, in a graphite die with a diameter of 15 mm.

2.5. Characterizations of the consolidated samples

2.5.1. Density

Density is an essential physical characteristic of any material with a mechanical application. It gives a good indication of the porosity and densification of the sintered samples. Following MPIF standards 42, 1998, the density of the sintered specimens was determined using the Archimedes water immersion method. The following formula was used to determine the sample density, shown in equation (1)[15].

$$Density(gm/cm^3) = \frac{Wight\ of\ sample\ in\ air}{Wight\ of\ sample\ in\ air - Wight\ of\ sample\ in\ water} \qquad \textbf{Equation (1)}$$

2.5.2. Phase structure and microstructure identification

To estimate the phase structure and composition of the prepared samples and investigate any new phases formed during the consolidation process. They were analyzed by x-ray diffraction analysis (XRD) utilizing x-ray diffractometer model x, pert PRO PANalytical with Cu kα radiation (λ = 0.15406 nm). The surface of the sintered samples was prepared for microstructure investigation by polishing and grinding using silicon carbide papers of varying grit (80, 400, 600, 800, 100, 1200, and 20000, respectively), and then finishing with alumina paste has 0.3 µm particle size.

The sintered metallographic structure was investigated using a scanning electron microscope (SEM) model TESCAN SEM VEGA3 and optical digital microscopy (OM) equipment ZEISS Ax10 Imager Alm.

2.5.3. Electrical and thermal conductivities

Electrical conductivity for all consolidated samples is measured using a PCE-COM20 conductivity meter at room temperature. The Wiedemann—Franz equation (2) determines the thermal conductivity.

$$\frac{\lambda}{\sigma T} = \frac{\pi^2 K_B^2}{3e^2} = L = 2.443 * 10^{-8} w\Omega/K^2 \qquad \textbf{Equation (2)}$$

Where λ is thermal conductivity (W/mK), σ is electrical conductivity $\Omega.m^{-1}$, T is the absolute temperature in degree Kelvin (293 k), K_B is Boltzmann constant, and L is Lorentz number[16].

2.5.4. Mechanical properties

Hardness

The hardness test is an essential mechanical characteristic for copper composite materials used in mechanical applications. In this work, the microhardness was estimated. A 500 g load and 10 seconds for microhardness was used. The

Vickers hardness tester type LalZhou Welyl, model HV-30MPTA, was used to measure consolidated samples' microhardness. For every specimen, the mean of three hardness readings was ascertained.

Tribological properties (wear rate and the friction coefficient)

The tribological test was applied to the polished samples using a (pin-on-disk) tester machine that works according to the SAE-J661 Standard Test [17]. The disk is made from tungsten carbide with a hardness of 75 HRC.

Depending on the sample's weight loss, the specific wear rate was detected using the same pin on the disk machine. It was measured under the same parameters mentioned above. The wear samples have a cylindrical shape with a diameter of 8 mm and a length of 10 mm. Before each test, the surface of the samples was polished and photographed by an optical microscope. The friction coefficient of the samples is detected under friction pressure of 0.4 and 0.7 MPa, with a 150-rpm rotation speed of the disc and sliding distance of 780 m during a test time of 15 minutes.

The specific wear rate [18]was calculated according to equation (3), where ΔV is the volume loss (mm^3), SD sliding distance (mm), and L is the load (N):

$$Specific\ wear\ rate\ (mm^3/N.m) = \frac{\Delta V}{SD*L} \qquad \textbf{Equation (3)}$$

The surface roughness of the samples was measured before and after the wear process using the Mitutoyo Surfest SJ-201. The worn surface of the wear-tested specimens (for both 0.4 MPa and 0.7 MPa) was analyzed and photographed using an optical microscope model (optical digital microscopy ZEISS Ax10 Imager Alm equipment). Then, the images of worn surfaces were processed analytically and graphically using Gwyddion software. Statistical analysis and Excel software were used to study the Abbott Firestone curves.

3. Results and discussions

3.1. Microstructure of the used powders

Figures (3) a, b, and c show the microstructure of the as-received copper, iron, and the prepared high-carbon ferrochromium powders, respectively. It is noted that copper has a dendritic structure ready by electric method; iron has a fine semicircular particle, while ferrochromium has an irregular big particle. Figures (3) d, e, and f represent the copper-coated MoS_2, Graphite, and recycled tungsten carbide powders, respectively. They all indicated the good nano Cu coating process and good adhesion between copper particles and the ceramic surfaces. In which auto-catalytic copper plating has been developed on activated and metalized conductive ceramic surfaces.

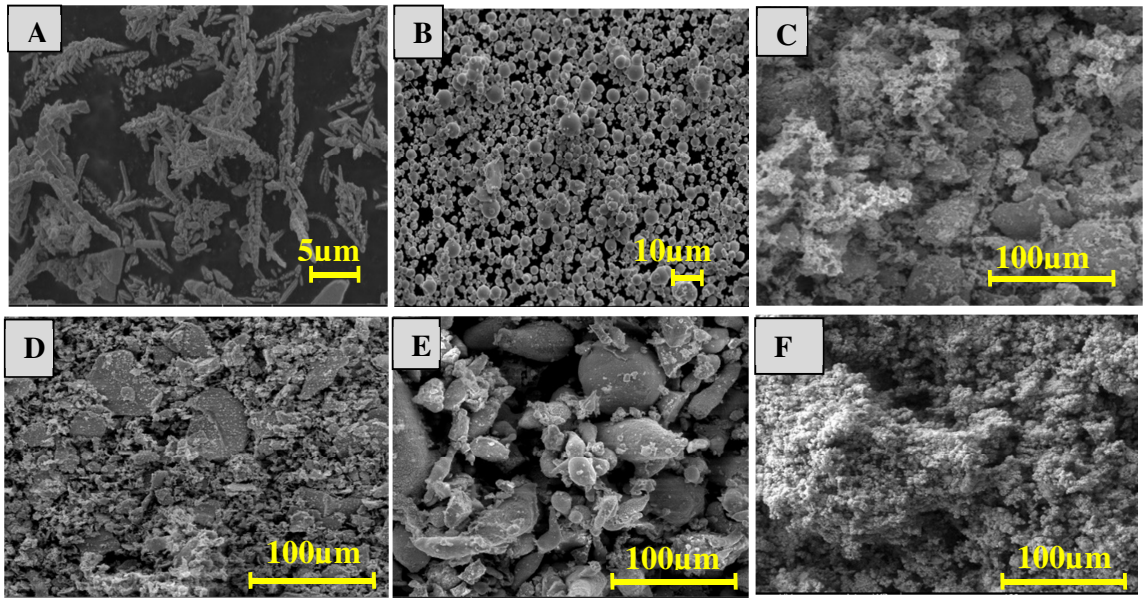

Figure (3): As received (a) Cu, (b) Fe, (C) Fe-Cr, and coated (d) MoS2, (E) C, (F) RWC powders

Figure (4) displays the XRD pattern of high-carbon ferrochromium powder. Two male peaks at 2Θ of 44.2° and 64.4°, which refer to the cubic CrFe, were recorded. This indicates the excellent and successful mechanical milling preparation process, which gives the required friction energy to form the ferrochromium alloy [18].

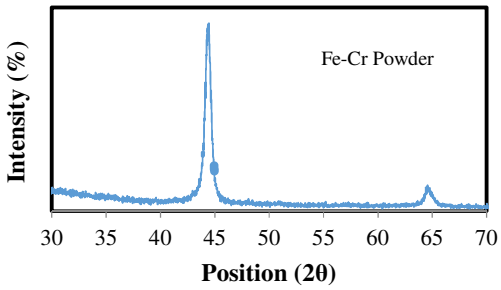

Figure (4): The XRD of the prepared ferrochromium powder

3.2 Microstructure of the consolidated samples

Figure (5) shows the microstructure investigation of the prepared Cu- composite materials. There are four mean areas: the white grey, which represents the copper matrix; the dark grey area, which belongs to iron; the black spots, which represent the graphite particles; and the white spots, which represent the recycled tungsten carbide particles. Finally, the MoS_2 appeared as a blocked dark grey area, as shown in the EDX analysis.

The Figure shows that all the additive materials are distributed homogeneously throughout the copper matrix[19]. This may be attributed to the suitable mechanical milling parameters, surface treatment, and coating of the ceramic reinforcement materials with the nano Cu layers [20].

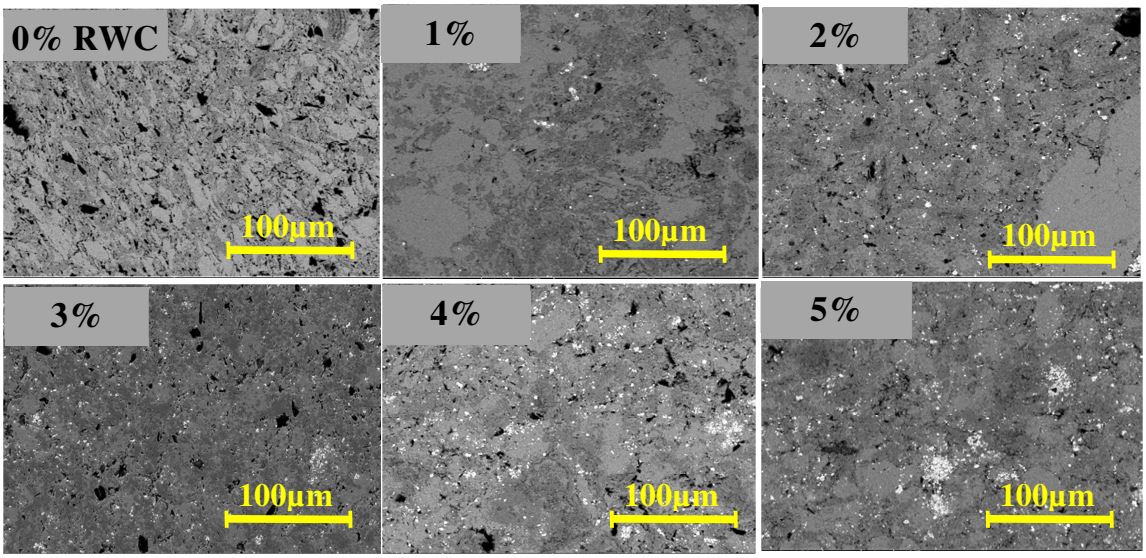

Figure (5): Microstructure under scan microscope of sintered samples at 1000X mag.

Scanning electron microscope images were recorded on the top, middle, and bottom areas to study their microstructure. Generally, the presence of RWC in the copper matrix helps in the grain refinement of the particles; this is because the RWC acts as an internal ceramic ball, causing the reduction of the particle's size, resulting in the improvement of the grain refinement and more densification with a homogeneous microstructure. However, it is observed that, for the high RWC percentages (4, 5 wt.%), some RWC aggregations were observed. This may be attributed to the high density of RWC particles (13.2 gm/cm^3) that causes some agglomerations. Also, RWC helps increase the dislocation, especially at high ratios, known as a crystallographic defect within the crystal structure that contains abrupt changes in the arrangement of atoms. This movement of dislocations allows particles to slide over each other, causing the agglomerations. Also, dislocation density increases with the decrease in particle size. The coating process of either graphite, RWC, or MoS_2 helps decrease the aggregations and grain growth of the particles.

The EDX analysis was carried out on a 3 wt.% RWC-Cu sample to analyze the distribution of all constituents in the Cu matrix, as shown in Figure (6) with their Tables. The copper coating distribution on the ceramic particle surfaces is uniform, with nearly every point containing all the composite elements. This indicates good mechanical milling and preparation conditions.

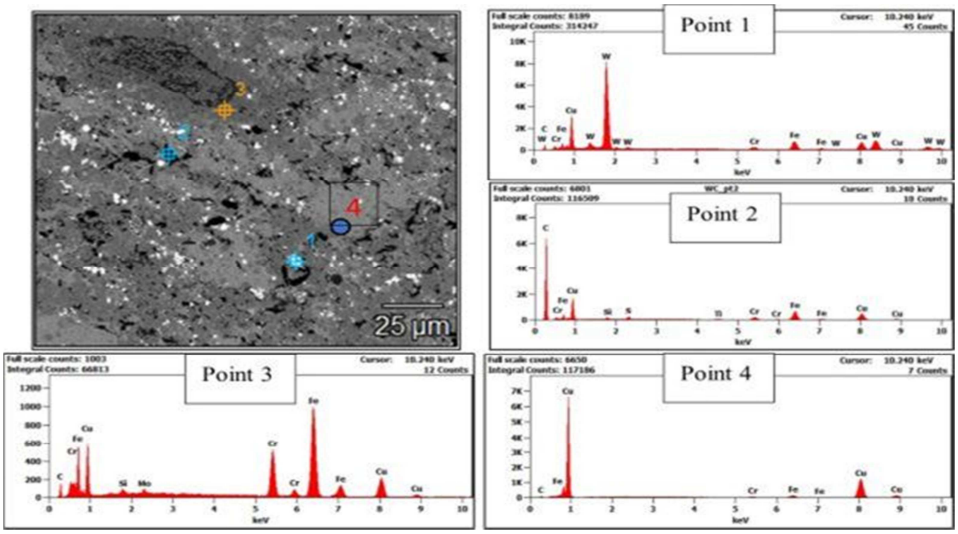

Figure (6): EDX of 3 wt.% RWC sample

3.3 XRD for the consolidated samples

The consolidated Cu samples are analyzed using XRD, as shown in Figure (7). The mean peaks of Cu, Fe, C, Ferro-chromium, MoS_2, and RWC are present. This is a good indication of the preparation process, where each metal, alloy, or material added remains without any change to play its role in the mechanical applications required. Also, no impurities were detected in the analysis.

It is observed that the XRD chart contains a peak at $76^{O,}$ which belongs to the Ferro-chromium alloy (Fe-Cr) formed by the mechanical alloying process. No new phases or compounds were formed during the preparation process. This may be attributed to the rapid hot-pressing consolidating technique. Hot-pressing is a densification process that involves simultaneously pressure and temperature and works in the plastic area of the constituents to achieve good interfacial contacts between them. Also, no oxide phases were recorded due to the controlled argon atmosphere mechanical milling process and vacuum hot-press technique [13].

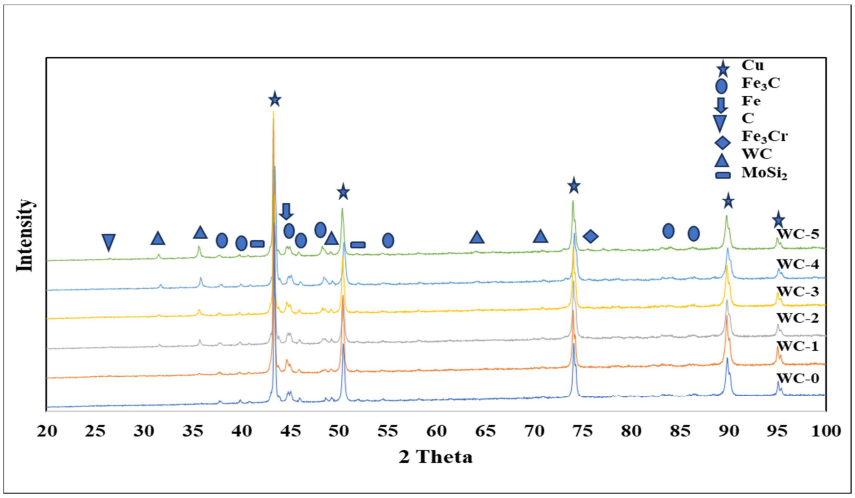

Figure (7): The XRD of the consolidated samples

3.4 Density measurement

Figure (8) represents the effect of the recycled WC powder addition on the density value of copper composites. The theoretical and actual densities of the prepared samples were recorded. There are two phenomena. The first is that the values of both the theoretical and actual densities are nearly close to each other. This may be attributed to the hot-pressing

consolidation process, where thermal energy improved the plasticity of metals and created suitable conditions for forming different bonds between the constituents during the hot-pressing technique [21].

So, nearly fully dense samples were obtained by applying heat and pressure simultaneously. Where the internal pores and voids are expelled from the samples. The second phenomenon is the gradual increase of the density of the samples by increasing the RWC ratio. This may be due to the higher density of RWC (14 gm/cm^3) and the excellent coating process of RWC, MoS_2, and graphite surfaces with the nano Cu layer, in which nearly complete capsulation of their surfaces was conducted, which has a positive effect on the homogenous distribution of the reinforcements in the Cu- matrix with no agglomerations created pores [1].

So, the surface energy between each one with the Cu-matrix was decreased. Consequently, good adhesion was established, which helps with high densification and improved wettability [22].

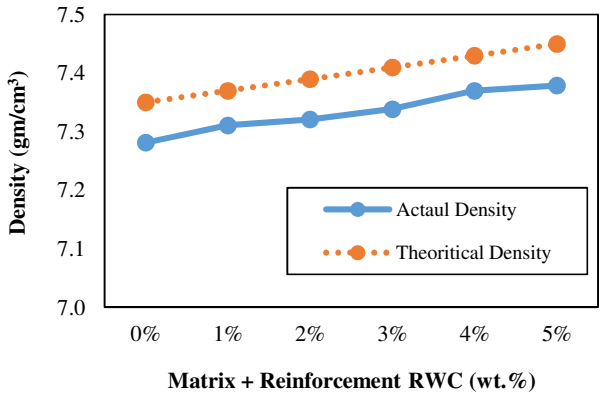

Figure (8): Actual and theoretical densities of consolidated samples

3.5 Electrical and thermal conductivities of consolidated samples

Figure (9) shows the effect of the RWC powders on the electrical conductivity of Cu-composites. It was noticed that it decreased gradually with the increase in the percentage of RWC. This is attributed to the low electrical conductivity values of the RWC due to its ceramic nature, which makes most ceramic materials dielectric. So, its addition decreases the motion of the electrons that are responsible for the conductivity. However, it must be mentioned that although the electrical conductivity decreases gradually, it is still in the conductance range of copper metal [3], which falls from 8.6 MS/m down to 7.3 MS/m, so the final product's electrical conductivity is still high. This can be explained by the coating process of the RWC, graphite (C), and molybdenum disulfide (MoS_2), with a nanolayer from copper metal, which helps significantly keep the electrical conductivity character of copper.

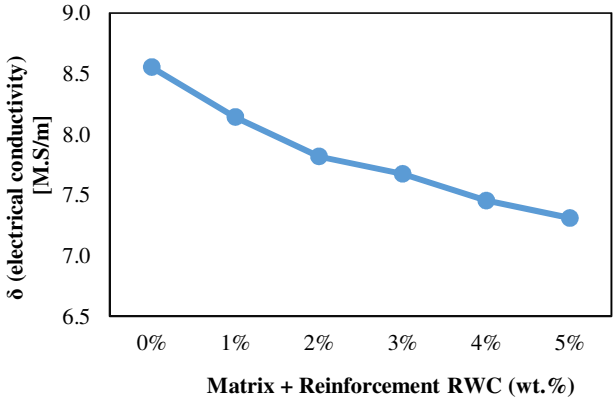

Figure (9): Electrical conductivity of all consolidated samples

Figure (10) shows the gradual decreases in the thermal conductivity of the prepared copper composites by increasing the ratio of the RWC particles. This is mainly due to RWC's lower thermal conductivity than copper's. So, reinforcing the copper matrix with RWC in a homogenous structure decreases the overall thermal conductivity of the samples; this is owing to the ceramic nature of RWC, which has nearly zero thermal conductivity. Also, the thermal conductivity of the prepared samples is still in the conductance range of copper, which is not significantly affected by RWC, as apparent from the curve in which thermal conductivity is decreased from about 62 w/mK down to 53 w/mK. This may be attributed to the excellent densification of the samples due to the hot-pressing technique used for the consolidation process and the coating

process of the ceramic reinforcements by the nano copper layer. As the presence of pores retards the motion of photons, which is responsible for thermal conductivity. Consequently, as the porosity is limited, there is no scattering for the photon, and the thermal conductivity of the final product is still high but with a higher mechanical property [23].

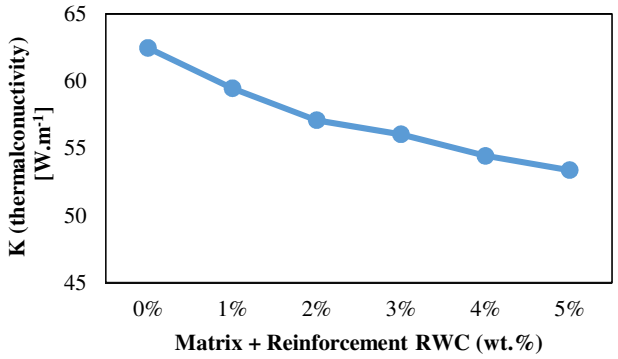

Figure (10): Thermal conductivity of all consolidated samples

3.6 Mechanical properties

3.6.1 Hardness measurements

Microhardness increases gradually with the increase in the RWC percentage, as shown in Figure (11). This is attributed to the higher RWC hardness than all the other composite constituents [24]. So, the excellent dispersion of RWC in a homogenous manner helps increase the hardness values. Also, the superb densification of samples and the high density positively affect hardness values. This is owing to the dendritic structure nature of the used copper, which helps in the excellent interaction of the particles under the hot-pressing technique. It must be mentioned that the superb coating process of all the ceramic reinforcements has a massive role in their homogeneity in the Cu matrix. This way, RWC particles are distributed all over the matrix and work as an internal network, giving a high strength at each point on the sample surface. RWC has a ceramic nature that improves the hardness of the samples. Although graphite is a soft material, there is a significant reduction in the hardness of the sintered samples. Yet, the high heating rate of the consolidation method results in more grain refinement of the particles. So, its softening nature doesn't affect the hardness significantly [25].

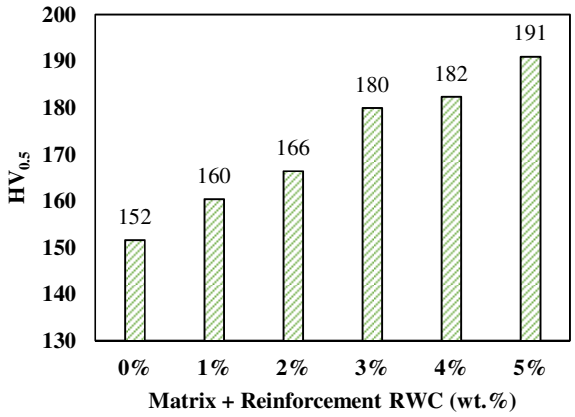

Figure (11): Micro-hardness of all consolidated samples

3.6.2 Tribological properties (wear rate and friction coefficient)

Figure (12) shows the effect of RWC additions on the specific wear rate of the consolidated Cu composites. Two different pressures, 0.4 and 0.7 MPa, are applied to study wear behavior. It is noted that there is a gradual decrease in the wear rate by increasing the RWC ratio. This is attributed to more than one reason: the excellent densification of the samples due to the hot-press technique that helps minimize the porosity percentage. This positively affects wear resistance, in which the presence of pores negatively affects the wear rate. Reinforcing the Cu matrix with self-lubricant materials such as MoS_2 and graphite helps slide the pin on the sample surface; consequently, the wear rate decreases [21]. Also, graphite has a low density; it floats on the sample surface, consisting of a trio layer that decreases the wear rate (R). Tungsten carbide particles have a ceramic nature with high hardness and low coefficient of friction; consequently, by increasing its ratio, the wear resistance is improved, especially when its distribution is homogenous, as shown from the microstructure [26].

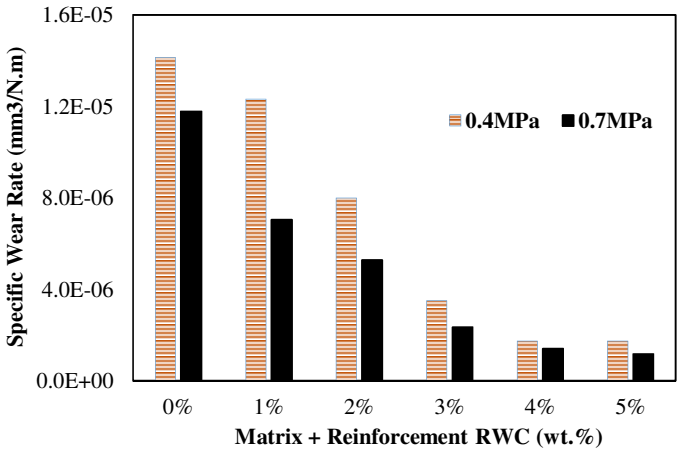

Figure (12): Specific wear rate of copper composite samples with different percentages of RWC under 0.4 & 0.7 MPa

Figure (13) presents the coefficient of friction of the samples under two different pressures of 0.4 and 0.7 MPa. The average value of the coefficient of friction is five measurements for each sample. The Figures show that the average coefficient of friction ranges between 0.3 to 0.5 under a pressure of 0.4 and between 0.3 to 0.6 under a pressure of 0.7. This coefficient of friction ratio is very suitable for alloys of this type, as they can be used in the manufacturing of brake pads, which require a coefficient of friction between 0.4 and 0.5.

Figure (13 a) shows that the average friction coefficient values increase for the 0% RWC sample (0.47). It decreases after adding RWC until it reaches the smaller value of (0.32) at 2%RWC, then increases gradually until it reaches the maximum value (0.5) at 5%RWC. Also, in Figure (13b), The average friction values increase at first (0.35) and decrease until they reach the smaller value for 2% RWC (0.33) and then increase until they reach the highest value for the 5% RWC (0.6) sample[27]. The higher COF value for the sample free from tungsten carbide may be due to the high ductility of Cu metal and the sticking characterization, which increases with the temperature during the friction process. The reinforcement material on the surface acts as a projection that protects the copper composite from having direct contact with the disk surface. Owing to the non-sticking ceramic properties of the RWC, it minimizes the contact area and reduces the adhesion of two mating surfaces [28].

However, as the percentage of tungsten carbide increases, some particles are dislocated during the friction process, and these particles leave gaps on the surface of the sample and also act as abrasive particles between the surface of the sample and the disc, which contributes to increasing the coefficient of friction again [29].

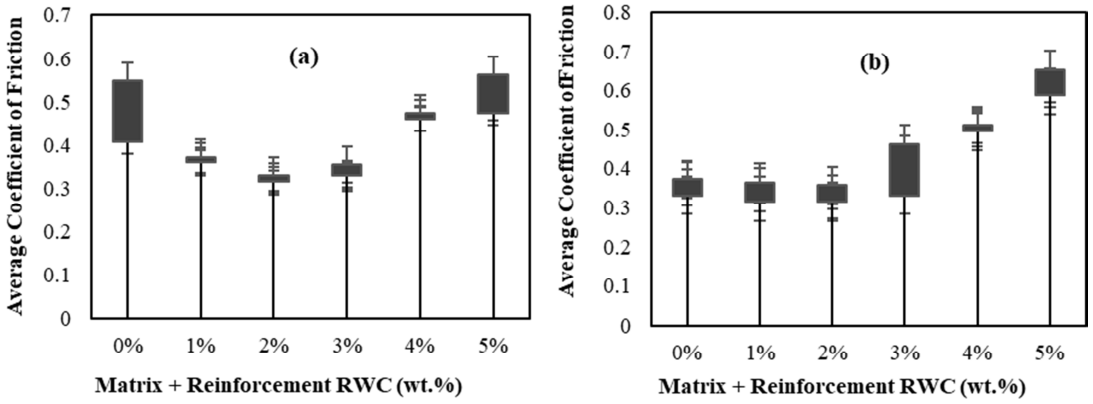

Figure (13): The coefficient of friction of copper composite samples with different percentages of RWC under 0.4 (A) & 0.7 (B) MPa

3.6.3 Optical and 3D worn surface of the prepared copper composites.

Worm surface under 0.4 MPa pressure

Figure (14) represents the optical microstructure and 3D pictures of worn surfaces of the different samples under pressure of 0.4 MPa. The visible worn lines on the worn surface samples from the adhesive wear mechanism were studied. The Figure

shows that the higher the percentage of tungsten carbide, the less worn lines appear on the surface. This indicates that the tungsten carbide made the surface harder and scratched hard during the wear process. This is due to the high hardness of RWC, which has good Cu-coating and homogenous distribution in the Cu matrix. The excellent adhesion of the coated Cu-layer on the RWC surface helps increase the surface's hardness, making it more difficult to scratch. In the 3D Figures, it was found that the surface converted from a grass-like shape to a bulky homogenous surface by increasing the tungsten carbide percentage. Also, the Figure presents how lubricant materials such as graphite and molybdenum sulfide are found in the sections worn down more quickly and show up as green patches in the 3D image. These materials have the ability to degrade rapidly, self-lubricant surface, with a self-lubricating nature, and lower density helps them to float on the sample surface, composing a trio-layer that causes sliding of the wear pin on the sample surface with a very low coefficient of friction.

Worm surface under 0.7 MPa pressure

Figure (15) shows the worn surfaces of the different samples under pressure of 0.7MPa using an optical microscope and 3D worn surfaces. The visible worn lines and scratches on the sample's surface were more observed due to the increased applied pressure. Here, it can be noticed that the surface experienced the reverse effect from the pressure of 0.4. When the applied load was increased from 0.4 to 0.7 MPa, and the percentage of tungsten carbide increased, the surface roughness was increased accordingly. This may be attributed to the softening nature of the Cu matrix. By applying a load of 0.7 MPa, the scratch of the worn surface increased due to the ceramic nature of the RWC particles impeded in the Cu- matrix is removed and expelled by the pin of the wear device under the applied higher load, so by increasing the load, the number of the removed RWC particles increases consequently the scratched lines increases the surface roughness. The second explanation is that the two surfaces' friction-dislodged tungsten carbide grains create voids that add to the roughness of the surface.

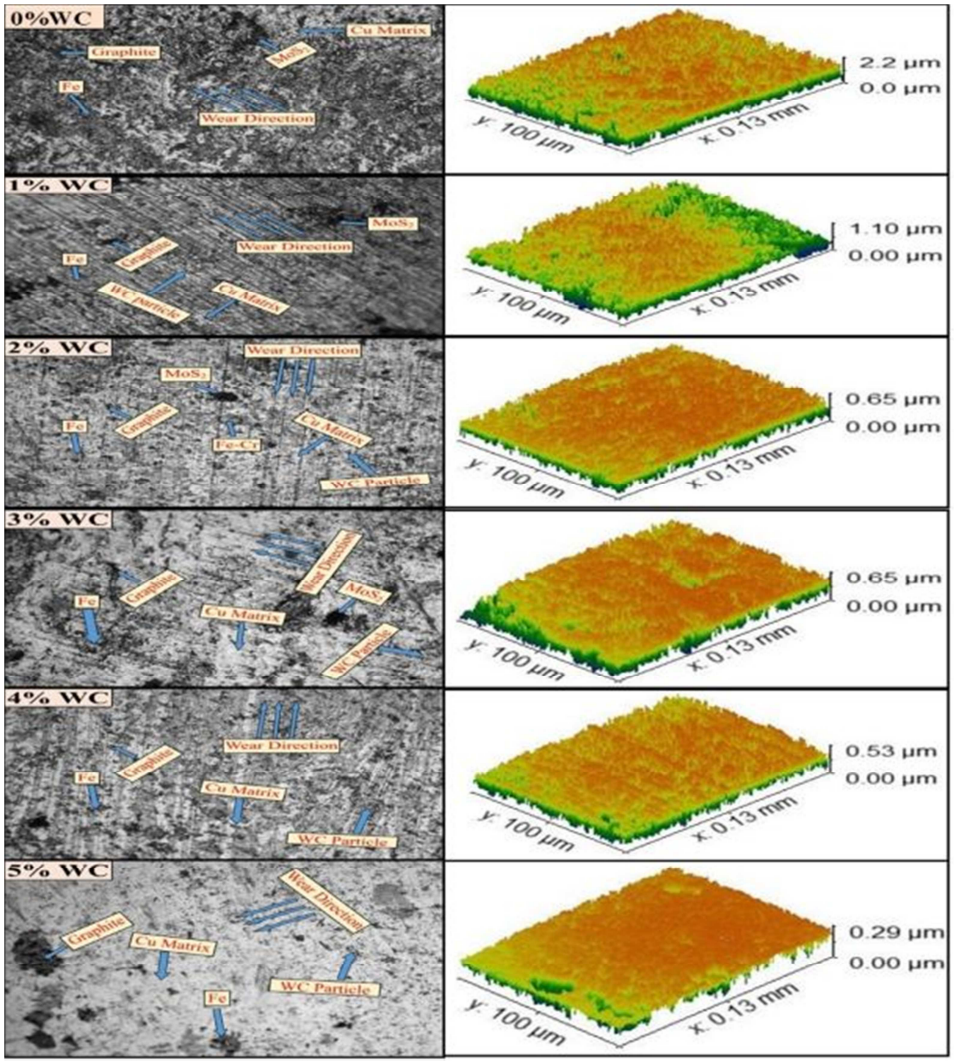

Figure (14): Optical microstructure and 3D worn surfaces after wear under 0.4 MPa

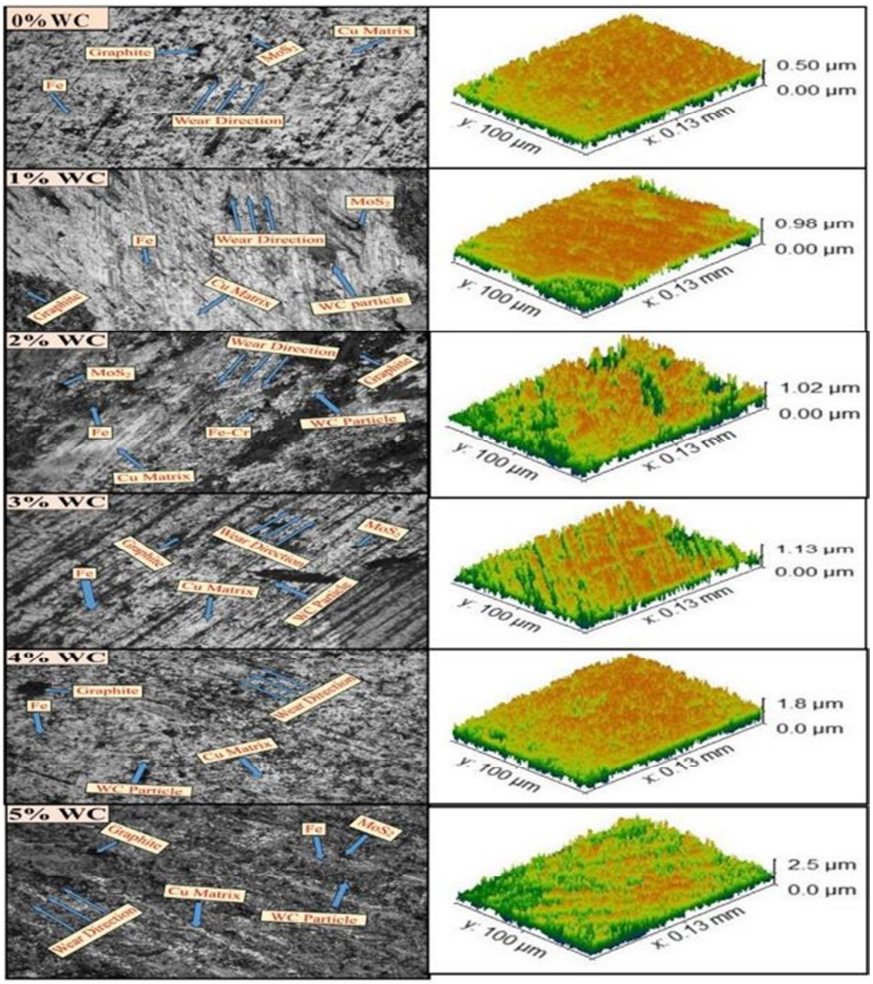

Figure (15): Optical microstructure and 3D worn surfaces after wear under 0.7 MPa

3.6.4 Surface roughness of the samples

Table (4) shows all polished samples' average surface roughness (Rz) before the wear process under 0.4 MPa and 0.7 MPa pressure. Which was measured using a Mitutoyo Surfest SJ-201 device, and the optical image of the surface was analyzed using Force Microscope (AFM) software. Surface roughness is an important character that determines how the spare parts can interact with each other during the working process under a specific load. The average surface roughness gradually increases from 0.2 up to 1.2 µm with the increase of the weight percentage of tungsten carbide. This may be attributed to the rigid ceramic nature of RWC particles and their big particle size. Also, the surface roughness increases by increasing the rate of the impeded RWC particles. Reinforcing the soft Cu matrix with the hard RWC particles with different surface energy causes the formation of heights and valleys in the sample surface, making the surface rough. This is because tungsten carbide particles are regarded as abrasive particles compared to the copper matrix, which is impeded within it.

Surface roughness indicates the physical geometry of surfaces and their relation to surface properties such as friction and the ability to manufacture high-quality products. The average surface roughness (Rz) started with a high value and diminished as the tungsten carbide ratio increased to 0.17. This may be due to the low effect of 0.4 MPa applied load on the sample surface, which is not enough to replace the RWC particles from the Cu surface. This indicates that the surface could hold together and not easily scratch under this 0.4 MPa pressure. So, the application parameters for the prepared Cu-composites are suitable up to 0.4 MPa.

The average surface roughness (Rz) started with a low value. Then, it increased as the tungsten carbide ratio increased to 1.7µm, which explains the increase in surface roughness with the rise in the percentage of tungsten carbide. Copper is a ductile metal with a soft nature, so it needs to be reinforced with a hard ceramic material such as RWC particles, which impeded the Cu matrix in a homogenous manner due to the coating process of the RWC surface.

However, a strong bond does not connect these carbide particles with the matrix. So, applying a load by a pin on the sample surface easily removes RWC particles from the surface. Consequently, increasing the RWC percentage increased the roughness.

Table (4): Surface roughness of sintered samples

Sample	before wear (µm)	under 0.4 MPa pressure (µm)	under 0.7 MPa pressure (µm)
Matrix + 0% RWC	0.209	1.645	0.376
Matrix + 1% RWC	0.522	0.695	0.701
Matrix + 2% RWC	0.7	0.477	0.785
Matrix + 3% RWC	0.602	0.488	0.993
Matrix + 4% RWC	0.658	0.374	1.433
Matrix + 5% RWC	1.242	0.17	1.716

The Abbott fire stone curves

The Abbott fire stone curves are called bearing area curves, and they describe a sample's surface texture. The curve can be found by drawing lines parallel to the datum and measuring the fraction of the line within the profile. Studying the sealing and bearing surface properties is essential [30-31].

The Abbott fire stone curves consider the analysis of profiles of samples in Figures (16 and 17) under different loads. To demonstrate the surface bearing while wearing. There are three zones in the curves [31].

Zone I: This represents the high peaks.

Zone II: Represents the exploitation zone (loading zone).

Zone III: Represents the voids zone.

Abbott fire stone curves of samples under 0.4 MPa pressure

Figure (16) shows the Abbott Firestone curves for the samples under pressure of 0.4 MPa. The results show that all samples have a large exploitation zone in which the least one is 88% and increases with increasing the tungsten carbide percentage until it reaches 96%, and this suggests that the addition of an abrasive substance, such as tungsten carbide, has high strengthening effect of the sample surface, this is more logic due to the high mechanical properties of RWC material.

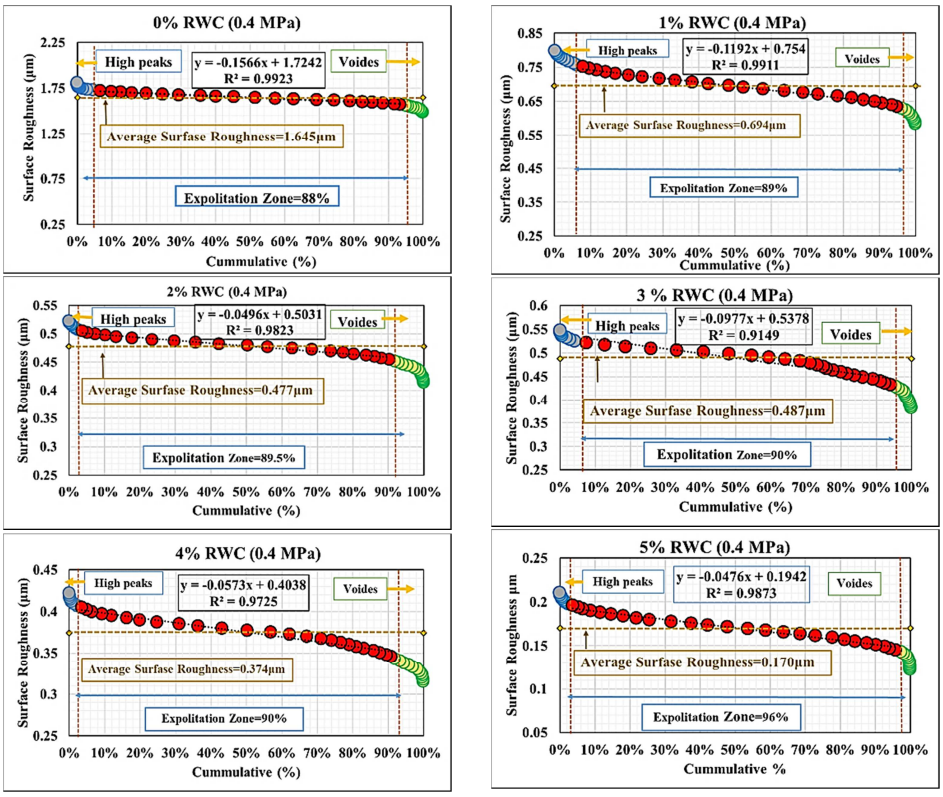

Figure (16): Abbott fire stone curves of surface roughness of Matrix + RWC reinforcement after wear test under pressure 0.4 MPa

Abbott fire stone curves of samples under 0.7 MPa pressure

Figure (17) shows the Abbott Firestone curves for the samples under pressure of 0.7 MPa. The results indicated that for all samples, the percentage of the exploitation zone was lower than that presented in Figure (16), as it began at 84% and reached 93%. This was attributed to the surface becoming more wriggling due to the increased load. Still, the observation showed that the bearing area increases as the percentage of tungsten carbide increases, indicating that it is greater at the bearing surface.

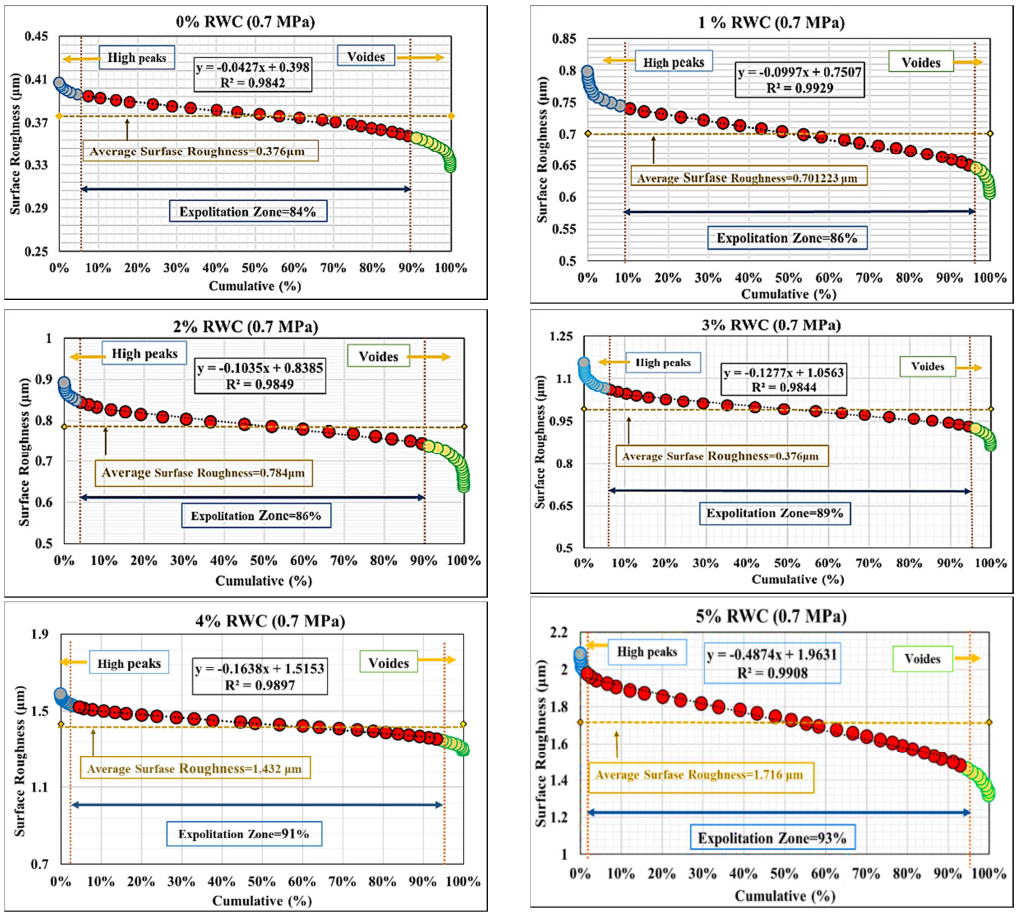

Figure (17): Abbott fire stone curves of surface roughness of matrix + RWC reinforcement after wear test under 0.7 MPa

4. Conclusion

In the present work, the copper matrix was firstly reinforced with fixed ratios from 8% high carbon ferrochromium (HC-FeCr), 20% iron (Fe), 10% graphite (C), and 2% (MoS_2). Then, different percentages from the RWC (1, 2, 3, 4, 5 wt.%) were added. All samples are consolidated in a Vertical Vacuum Hot Press Furnace under the pressure of 15 MPa at 1010 ^{C} for 15 minutes.

The results indicated that:

- A Cu—Fe—graphite—FeCr—MoS_2 /RWC composite was prepared using powder metallurgy and hot-pressing techniques.
- adding Fe, High-carbon ferrochromium alloy, graphite, and MoS_2 enhances the mechanical properties of the Cu-matrix.
- The microstructure shows no pores due to excellent wettability after coating the ceramic powders with a nano copper layer on their surfaces by electroless deposition technique.
- The excellent homogenous distribution of RWC particles in the copper matrix composites.
- Nearly fully dense samples were obtained by applying the Hot-press technique (heat with pressure at the same time) in which the relative density reached 99 %.
- The increase of RWC particles decreased the electrical and thermal conductivities.
- The hardness of the samples increased with the increase in the RWC particles.

- The specific wear rate decreases with the increasing RWC particles.
- The surface roughness of the prepared samples before the wear test was increased with increasing RWC ratio.
- Increasing the RWC ratio decreased the surface roughness of the prepared samples after the wear test under 0.4 MPa load.
- Increasing the RWC ratio increased the surface roughness of the prepared samples after the wear test under 0.7 MPa load.
- 3 wt.% RWC - Cu composite offers optimal hardness, wear resistance, and friction performance, making it the best choice for brake pad applications. Its improved hardness enhances durability, while its low wear rate ensures long-term performance. Additionally, its friction coefficient (~0.32–0.33) falls within the ideal range for braking systems, providing consistent and reliable operation under various load conditions.

5. Conflict of Interests

The authors have no relevant financial or nonfinancial interests to disclose and have declared no conflicts of interest regarding this work.

6. Acknowledgement

I am grateful to all the teachers who assisted me in completing this task by giving me the essential tools in CMDRI and Faculty of Engineering, Minia University, without which I could not have completed it. And special thanks to Dr. Supervisor Asaad A. Mazen, who passed away during this work. Many thanks to Professors A. I. Z. Farahat and H. M. Zidan for their help analyzing the data.

7. Data Availability

Correspondence and requests for materials should be addressed to Ahmed O. Abdel-Mawla.

8. Ethical Standards

This paper has no potential conflicts of interest, and the research didn't involve any human participants and/or animals.

9. Funding

No funding was received to conduct this study.

10. References

[1] C. Chen, D. Li, Z. Zhai, C. Sun, and W. Chen, "Micro-/nano-scale WC particle-reinforced Cu-based composite preparation and property study," *AIP Adv*, vol. 13, no. 8, Aug. 2023, doi: 10.1063/5.0160981.

[2] H. Zhou *et al.*, "Effects of ZrO2 crystal structure on the tribological properties of copper metal matrix composites," *Tribol Int*, vol. 138, pp. 380–391, Oct. 2019, doi: 10.1016/j.triboint.2019.06.005.

[3] B. M. Girish, B. B., B. M. Satish, and D. R. Somashekar, "Electrical Resistivity and Mechanical Properties of Tungsten Carbide Reinforced Copper Alloy Composites," *International Journal of Composite Materials*, vol. 2, no. 3, pp. 37–43, Aug. 2012, doi: 10.5923/j.cmaterials.20120203.04.

[4] L. Han *et al.*, "Effect of WC nanoparticles on the thermal stability and mechanical performance of dispersion-reinforced Cu composites," *Scr Mater*, vol. 222, Jan. 2023, doi: 10.1016/j.scriptamat.2022.115030.

[5] D. Rajesh, P. Anand, N. Lenin, V. K. Bupesh Raja, K. Palanikumar, and V. Balaji, "Investigations on the mechanical properties of tungsten carbide reinforced aluminium metal matrix composites by stir casting," in *Materials Today: Proceedings*, Elsevier Ltd, 2020, pp. 3618–3620. doi: 10.1016/j.matpr.2021.01.634.

[6] D. Gu and Y. Shen, "Microstructures and properties of direct laser sintered tungsten carbide (WC) particle reinforced Cu matrix composites with RE - Si - Fe addition: A comparative study," *J Mater Res*, vol. 24, no. 11, pp. 3397–3406, Nov. 2009, doi: 10.1557/jmr.2009.0419.

[7] T. M. Vidyuk *et al.*, "Synthesis of Tungsten Carbides in a Copper Matrix by Spark Plasma Sintering: Microstructure Formation Mechanisms and Properties of the Consolidated Materials," *Materials*, vol. 16, no. 15, Aug. 2023, doi: 10.3390/ma16155385.

[8] H. Ahmadian, A. Fouly, T. Zhou, A. S. Kumar, A. Fathy, and G. Weijia, "Investigating the valence balance of adding Nano SiC and MWCNTs on the improvement properties of copper composite using mechanical alloying and SPS techniques," *Diam Relat Mater*, vol. 145, May 2024, doi: 10.1016/j.diamond.2024.111113.

[9] A. Sadoun, A. Ibrahim, and A. W. Abdallah, "Fabrication and evaluation of tribological properties of Al2O3 coated Ag reinforced copper matrix nanocomposite by mechanical alloying," *Journal of Asian Ceramic Societies*, vol. 8, no. 4, pp. 1228–1238, 2020, doi: 10.1080/21870764.2020.1841073.

[10] A. O. Abdel-Mawla, M. A. Taha, O. A. El-Kady, and A. Elasyed, "Recycling of WC-TiC-TaC-NbC-Co by zinc melt method to manufacture new cutting tools," *Results Phys*, vol. 13, Jun. 2019, doi: 10.1016/j.rinp.2019.02.028.

[11] G. Fadel *et al.*, "Evaluation of corrosion and wear features of Al matrix reinforced with particles (SiC+Y2O3) coated with either nano-Ag/Ni or nano/Ag/Cu," *Egypt J Chem*, vol. 67, no. 8, pp. 137–155, Jan. 2024, doi: 10.21608/EJCHEM.2024.247764.8845.

[12] H. M. Yehia, F. Nouh, and O. El-Kady, "Effect of graphene nano-sheets content and sintering time on the microstructure, coefficient of thermal expansion, and mechanical properties of (Cu /WC –TiC-Co) nano-composites," *J Alloys Compd*, vol. 764, pp. 36–43, Oct. 2018, doi: 10.1016/j.jallcom.2018.06.040.
[13] A. Abu-Oqail, A. Wagih, A. Fathy, O. Elkady, and A. M. Kabeel, "Effect of high energy ball milling on strengthening of Cu-ZrO2 nanocomposites," *Ceram Int*, vol. 45, no. 5, pp. 5866–5875, Apr. 2019, doi: 10.1016/j.ceramint.2018.12.053.
[14] A. T. Hamed, E. S. Mosa, A. Mahdy, I. G. El-Batanony, and O. A. Elkady, "Preparation and evaluation of cu-zn-gnss nanocomposite manufactured by powder metallurgy," *Crystals (Basel)*, vol. 11, no. 12, Dec. 2021, doi: 10.3390/cryst11121449.
[15] J. R, *Testing method for apparent porosity, water absorption specific gravity of refractory bricks*. Japanese Industrial Standards, 1992.
[16] O. El-Kady, H. M. Yehia, and F. Nouh, "Preparation and characterization of Cu/(WC-TiC-Co)/graphene nano-composites as a suitable material for heat sink by powder metallurgy method," *Int J Refract Metals Hard Mater*, vol. 79, pp. 108–114, Feb. 2019, doi: 10.1016/j.ijrmhm.2018.11.007.
[17] E. F. EL-kashif, S. A. Esmail, O. A. M. Elkady, B. S. Azzam, and A. A. Khattab, "Influence of carbon nanotubes on the properties of friction composite materials," *J Compos Mater*, vol. 54, no. 16, pp. 2101–2111, Jul. 2020, doi: 10.1177/0021998319891772.
[18] Z. Abidin, T. Nugroho, R. Tri Indrawati, E. Safriana, and F. Tono Putri, "Wear Rate Analysis Due to Dry Sliding Contact of Modified Rail to Increase Life Time in Air Blow Machine," 2022. [Online]. Available: https://jurnal.polines.ac.id/index.php/rekayasa
[19] M. I. Elamy, M. Abd Elaziz, M. A. Al-Betar, A. Fathy, and M. Elmahdy, "Enhanced random vector functional link based on artificial protozoa optimizer to predict wear characteristics of Cu-ZrO2 nanocomposites," *Results in Engineering*, vol. 24, Dec. 2024, doi: 10.1016/j.rineng.2024.103007.
[20] M. Eid, S. Kaytbay, O. Elkady, and A. El-Assal, "Microstructure and mechanical properties of CF/Al composites fabricated by hot coining technique," *Ceram Int*, vol. 47, no. 15, pp. 21890–21904, Aug. 2021, doi: 10.1016/j.ceramint.2021.04.207.
[21] F. Hamid, A. Elsayed, O. Elkady, A. EL-Nikhaily, and A. Essa, "Synthesis and Evaluation of Strengthened Copper with 3 wt. % TiC and/ or Al2O3 Prepared By SPS Technique," *Journal of Petroleum and Mining Engineering*, vol. 0, no. 0, pp. 41–50, May 2021, doi: 10.21608/jpme.2021.68894.1079.
[22] M. A. Elmaghraby, H. M. Yehia, O. A. Elkady, and A. Abu-Oqail, "Effect of Graphene Nano-Sheets Additions on the Microstructure and Wear Behavior of Copper Matrix Nano-Composite," 2018.
[23] H. M. Yehia, O. El-Kady, and A. Abu-Oqail, "Effect of diamond additions on the microstructure, physical and mechanical properties of WC- TiC- Co/Ni Nano-composite," *Int J Refract Metals Hard Mater*, vol. 71, pp. 198–205, Feb. 2018, doi: 10.1016/j.ijrmhm.2017.11.018.
[24] D. Madhesh, K. Jagatheesan, T. Sathish, and K. Balamanikandasuthan, "Microstructural and mechanical properties of copper matrix composites," in *Materials Today: Proceedings*, Elsevier Ltd, 2020, pp. 1437–1441. doi: 10.1016/j.matpr.2020.06.600.
[25] H. M. Yehia, A. Abu-Oqail, M. A. Elmaghraby, and O. A. Elkady, "Microstructure, hardness, and tribology properties of the (Cu/MoS2)/graphene nanocomposite via the electroless deposition and powder metallurgy technique," *J Compos Mater*, vol. 54, no. 23, pp. 3435–3446, Sep. 2020, doi: 10.1177/0021998320916528.
[26] P. K. Deshpande and R. Y. Lin, "Wear resistance of WC particle reinforced copper matrix composites and the effect of porosity," *Materials Science and Engineering: A*, vol. 418, no. 1–2, pp. 137–145, Feb. 2006, doi: 10.1016/j.msea.2005.11.036.
[27] E. Ghandourah *et al.*, "Comprehensive investigation of the impact of milling time on microstructural evolution and tribological properties in Mg-Ti-SiC hybrid composites," *Mater Today Commun*, vol. 38, Mar. 2024, doi: 10.1016/j.mtcomm.2023.107835.
[28] B. M. Santhosh Kumar and D. P. Girish, "Friction and Wear Behaviour of Tungsten Carbide and e Glass Fibre reinforced Al7075 based Hybrid composites," in *IOP Conference Series: Materials Science and Engineering*, Institute of Physics Publishing, Jul. 2018. doi: 10.1088/1757-899X/390/1/012002.
[29] M. Madej, "Tungsten Carbide as an Addition to High Speed Steel Based Composites," in *Tungsten Carbide - Processing and Applications*, InTech, 2012. doi: 10.5772/51243.
[30] M. C. Salcedo, I. B. Coral, and G. V. Ochoa, "Characterization of surface topography with Abbott Firestone curve," *Contemporary Engineering Sciences*, vol. 11, no. 68, pp. 3397–3407, 2018, doi: 10.12988/ces.2018.87319.
[31] E. H. El-Shenawy and A. I. Z. Farahat, "Surface quality and dry sliding wear behavior of AZ61Mg alloy using Abbott firestone technique," *Sci Rep*, vol. 13, no. 1, Dec. 2023, doi: 10.1038/s41598-023-39413-x.